Supporting information

Coordination engineering in Nd^{3+}-doped silica glass for improving repetition rate of 920 nm ultrashort-pulse fiber laser

Yafei Wang[1, †], Yinggang Chen[1, 2, †], Shikai Wang[1, *], Meng Wang[1], Lei Zhang[1], Suya Feng[1], Fei Yu[1, 3], Guoping Dong[4], Lei Wen[1], Danping Chen[1], Chunlei Yu[1, 3, *], Lili Hu[1, 3, *]

[1]*Key Laboratory of Materials for High Power Laser, Shanghai Institute of Optics and Fine Mechanics, Chinese Academy of Sciences, Shanghai 201800, China*

[2]*University of Chinese Academy of Sciences, Beijing 100039, China*

[3]*Hangzhou Institute for Advanced Study, University of Chinese Academy of Sciences, Hangzhou 310024, China*

[4]*State Key Laboratory of Luminescent Materials and Devices, School of Materials Science and Engineering, South China University of Technology, Guangzhou 510640, China*

[†]*Equal contribution*

[*]*Corresponding author, woshiwsk@163.com; sdycllcy@163.com; hulili@siom.ac.cn*

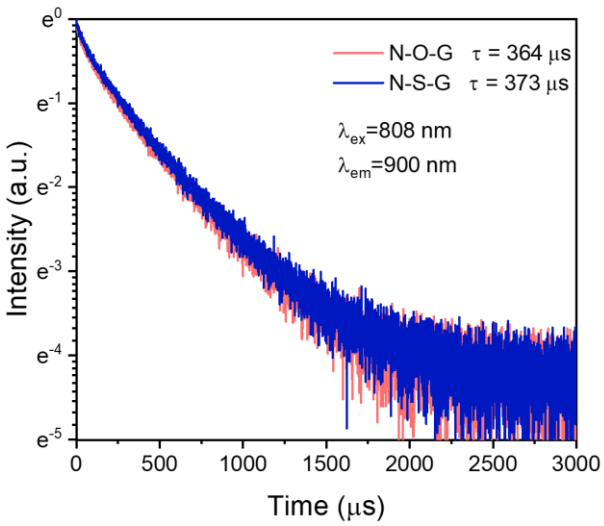

Figure S1 Decay curves of $^4F_{3/2}$ level of N-O-G and N-S-G.

Figure S1 shows the measured decay curves for the $^4F_{3/2}$ level of N-O-G and N-S-G. Fitted by single exponential decay, the lifetimes of N-O-G and N-S-G were identified to be 364 μs and 373 μs, respectively.

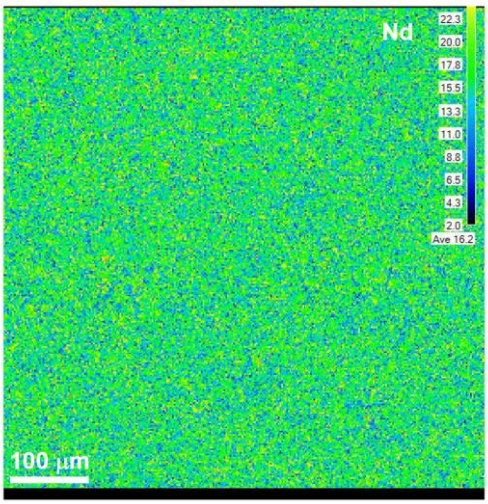

Figure S2 EPMA mapping image of Nd

Figure S2 shows the measured EPMA mapping image of Nd, which indicate the Nd present homogenous distribution in micro-scale. Combined with the TEM analyses, it can conclude that the glasses maintain high homogeneity after the introduction of sulfur.

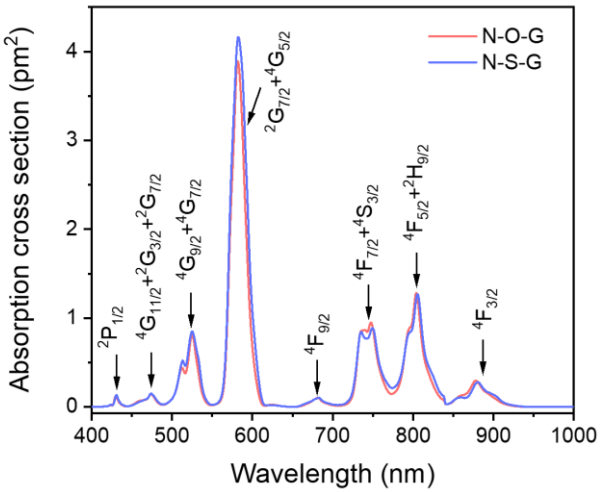

Figure S3 Absorption spectra of N-O-G and N-S-G.

Figure S3 shows the absorption spectra of N-O-G and N-S-G in the 400–1000 nm range. Eight characteristic absorption bands of Nd^{3+} are observed and the corresponding energy level are marked in the spectra. The peaks of these emission band of N-S-G present a slight red-shift compared to those of N-O-G. This provides an additional support for the variation in the environment surrounding Nd^{3+} after co-doping with

sulfur.

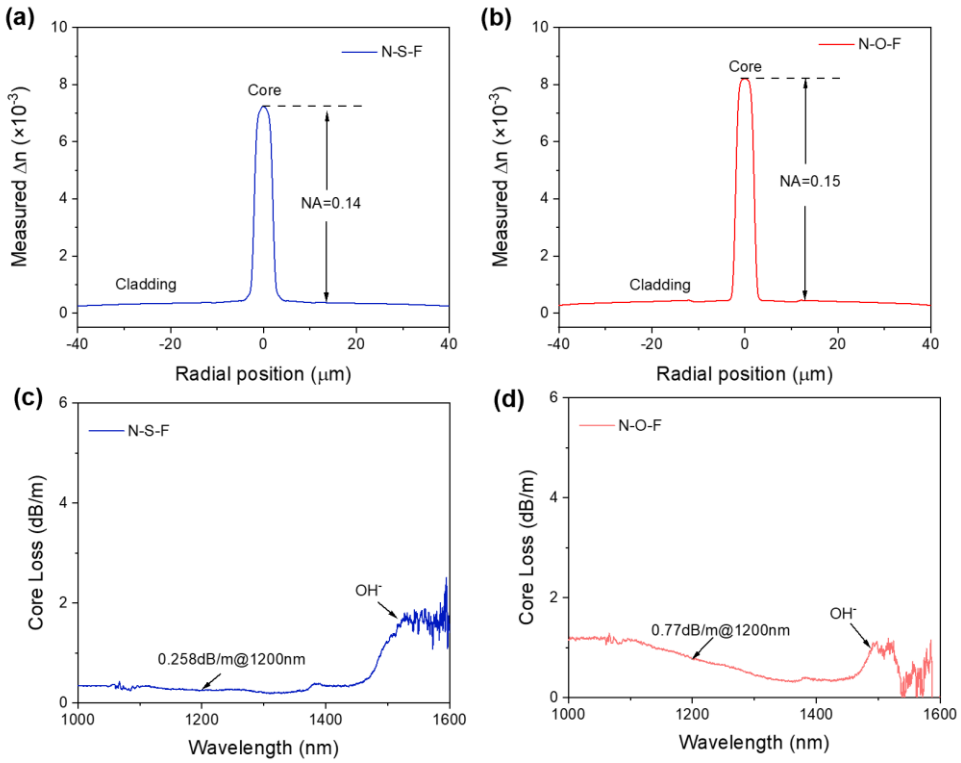

Figure S4 Refractive index profiles of (a) N-S-F and (b) N-O-F. Transmission loss of (c) N-S-F and (d) N-O-F, respectively.

Figure S4 (a-b) shows the refractive index profile of N-S-F and N-O-F, respectively. The refractive index difference (Δn) between the core and silica cladding for N-S-F is approximately 7×10^{-3}, and the core NA can be calculated to be 0.14. For N-O-F, the Δn is approximately 8×10^{-3}, and the NA is 0.15. Figure S4 (c-d) show the measured transmission loss of N-S-F and N-O-F, respectively. The propagation loss at 1200 nm for N-S-F and N-O-F are 0.26 dB/m and 0.77 dB/m, respectively. It is necessary to mention that although the background loss is higher than that of a fiber fabricated by the classical modified chemical vapor deposition (MCVD) method, it does not affect the laser performance as only a centimeter-scale fiber length needs to be used because of high pump absorption. We anticipate that the background loss could be further reduced by optimizing the M-Sol-Gel process, for example, by adopting a higher-purity raw material to exclude impurities absorption, such as transition-metal ions.

Figure S5 Experimental setup for fiber ASE measurement.

Figure S5 shows the experimental setup for fiber ASE measurement. A fiber-pigtailed 808-nm LD was used as the pump source, which is coupled into Nd-doped silica fiber using WDM. The forward ASE was coupled into OSA by a matched Hi-780 passive fiber. For comparison, pump power was fixed at 200 mW and total 40 dB pump absorption was provided by N-S-F/N-O-F to ensure adequate pump absorption. The lengths of N-S-F and N-O-F were slightly adjusted according to their absorption coefficient at 808 nm.

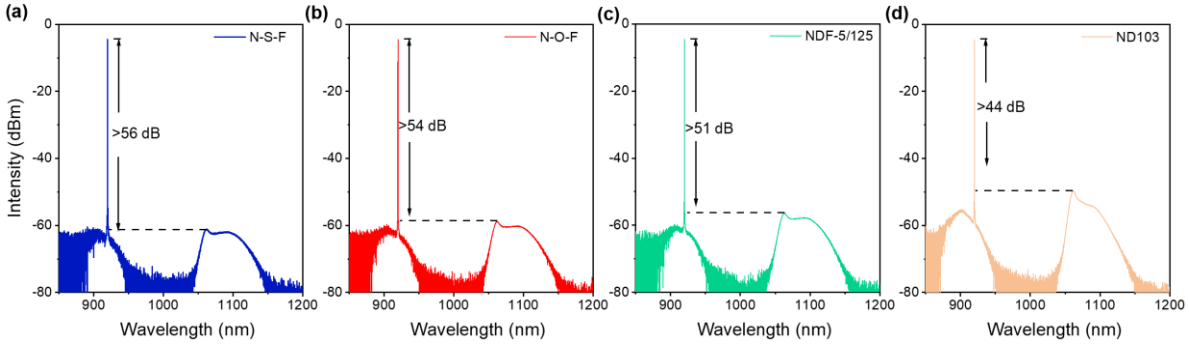

Figure S6 920-nm laser spectra generated using (a) N-S-F, (b)N-O-F, (c) PM-NDF-5/125 (Nufern) and (d) ND103 (Coractive).

Figure S6(a-d) show the detailed 920 nm laser spectra by N-S-F, N-O-F, PM-NDF-5/125 and ND103, respectively. The peak intensities at 920 nm were the same because the laser power injected into the OSA were attenuated to identical value. The laser SNR values for N-S-F, N-O-F, PM-NDF-5/125 and ND103 were greater than 56, 54, 51 and 44 dB, respectively.

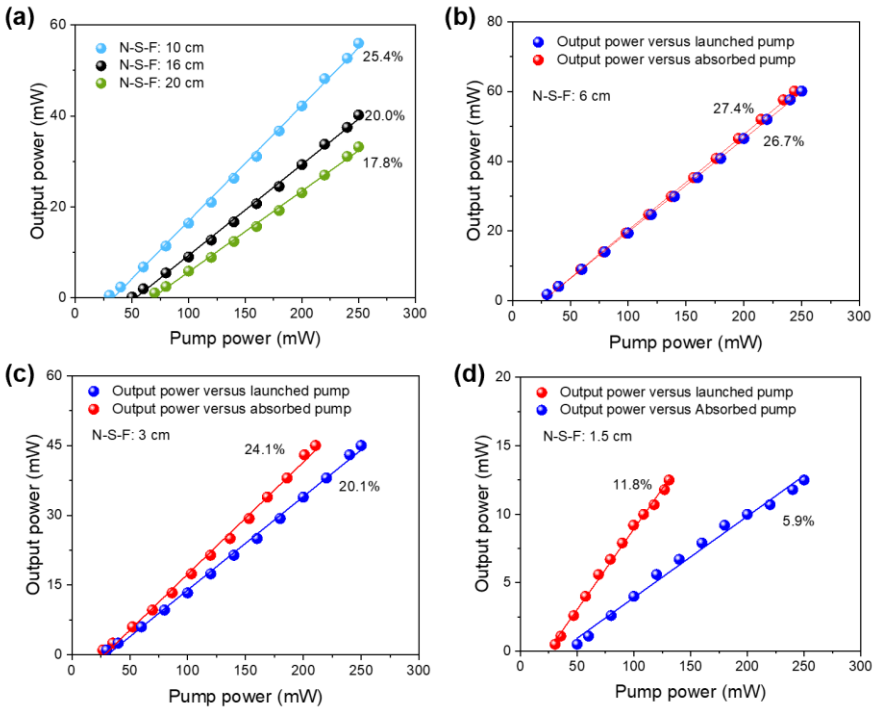

Figure S7 920-nm laser output power versus launched pump power and absorbed pump power using N-S-F with lengths of (a) 10-cm, 16-cm and 20-cm, (b) 6-cm, (c) 3-cm, and (d) 1.5-cm N-S-F.

Figure S7 shows the 920 nm laser output power versus the pump power at different N-S-F fiber lengths. For the fiber lengths greater than 6 cm, almost all the launched pump power was completely absorbed. The slope efficiencies decreased monotonically from 27.4 % to 17.8% when the fiber length was increased from 6 cm to 20 cm. The reason for this is because the re-absorption at 920 nm increases with increasing fiber length. Furthermore, when the fiber length was further shortened, the slope efficiencies decreased because the pump power was insufficiently absorbed. Moreover, it is worth mentioning that the slope efficiency still reaches 11.8% for 1.5-cm N-S-F.

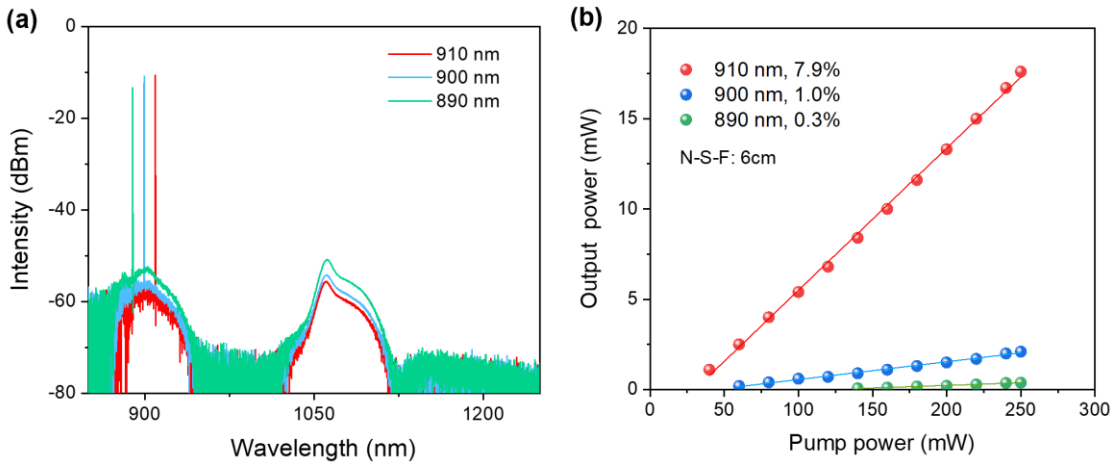

Figure S8 (a) 890 nm-910 nm laser spectra by N-S-F and (b) laser output power as the function of pump power.

Based on the same CW laser configuration at 920 nm, we further explored the lasing performance at 890, 900 and 910 nm by taking three pairs of FBGs centered at these wavelengths. Referring to the fiber length with an optimal laser efficiency of 920 nm, the fiber length was fixed at 6-cm. Differently, the available reflectivity of LR-FBGs at these three wavelengths are around 80%, a little higher compared to the 920 nm. Figure S8a shows the recorded laser spectra; notably, the laser oscillations could be rendered by our N-S-F but the laser efficiencies decreased quickly compared to those at 920 nm (Figure S8b). Especially for 900 nm and 890 nm, the efficiencies decreased to 1.0% and 0.3%, respectively. Such low efficiencies are mainly ascribed to the stronger re-absorption at 900 nm and 890 nm.